JCI The Journal of Clinical Investigation

Tumor infiltrating $BRAF^{V600E}$-specific CD4 T cells correlated with complete clinical response in melanoma

Joshua R. Veatch, … , William W. Kwok, Stanley R. Riddell

J Clin Invest. 2018. https://doi.org/10.1172/JCI98689.

Concise Communication In-Press Preview **Immunology** **Oncology**

T cells specific for neoantigens encoded by mutated genes in cancers are increasingly recognized as mediators of tumor destruction after immune checkpoint inhibitor therapy or adoptive cell transfer. Unfortunately, most neoantigens result from random mutations and are patient specific, and some cancers contain few mutations to serve as potential antigens. We describe a patient with stage IV acral melanoma who obtained a complete response following adoptive transfer of tumor infiltrating lymphocytes (TIL). Tumor exome sequencing surprisingly revealed less than 30 somatic mutations, including oncogenic BRAF V600E. Analysis of the specificity of TIL identified rare CD4 T cells specific for BRAFV600E and diverse CD8 T cells reactive to non-mutated self-antigens. These specificities increased in blood after TIL transfer and persisted long term suggesting they contributed to the effective antitumor immune response. Gene transfer of the $BRAF^{V600E}$-specific T cell receptor (TCR) conferred recognition of class II MHC positive cells expressing the BRAF mutation. Therapy with TCR engineered $BRAF^{V600E}$-specific $CD4^+$ T cells may have direct antitumor effects and augment $CD8^+$ T cell responses to self and/or mutated tumor antigens in patients with BRAF mutated cancers.

Tumor infiltrating $BRAF^{V600E}$-specific CD4 T-cells correlated with complete clinical response in melanoma

Joshua R. Veatch[1]*, Sylvia M. Lee[2], Matthew Fitzgibbon[3], I-Ting Chow[4], Brenda Jesernig[1], Tom Schmitt[1], Ying Ying Kong[4], Julia Kargl[1,5], A. McGarry Houghton[1], John A. Thompson[2], Martin McIntosh[3], William W. Kwok[4], Stanley R. Riddell[1]

Affiliations:

1) Clinical Research Division, Fred Hutchinson Cancer Research Center, Seattle, WA, USA 98109

2) Division of Medical Oncology, University of Washington, Seattle, WA, USA 98102

3) Public Health Sciences, Fred Hutchinson Cancer Research Center, Seattle, WA, USA 98109

4) Benaroya Research Institute, Seattle, WA, USA 98101

5) Institute of Experimental and Clinical Pharmacology, Medical University of Graz, 8010 Graz, Austria.

*Corresponding author: jveatch@fredhutch.org

(206)667-5108

Mailstop D3-100

1100 Fairview Ave N, Seattle, WA 98109

Conflicts of interest: S.R.R. has received research grants and has equity interest in Juno Therapeutics. J.R.V., S.M.L. and S.R.R. are inventors on a pending patent related to this work (US Provisional Application No. 62/544,695). No other conflicts of interest are declared.

Abstract

T cells specific for neoantigens encoded by mutated genes in cancers are increasingly recognized as mediators of tumor destruction after immune checkpoint inhibitor therapy or adoptive cell transfer. Unfortunately, most neoantigens result from random mutations and are patient specific, and some cancers contain few mutations to serve as potential antigens. We describe a patient with stage IV acral melanoma who obtained a complete response following adoptive transfer of tumor infiltrating lymphocytes (TIL). Tumor exome sequencing surprisingly revealed less than 30 nonsynonymous somatic mutations, including oncogenic BRAF V600E. Analysis of the specificity of TIL identified rare CD4 T cells specific for BRAF V600E and diverse CD8 T cells reactive to non-mutated self-antigens. These specificities increased in blood after TIL transfer and persisted long term suggesting they contributed to the effective antitumor immune response. Gene transfer of the $BRAF^{V600E}$-specific T cell receptor (TCR) conferred recognition of class II MHC positive cells expressing the BRAF mutation. Therapy with TCR engineered $BRAF^{V600E}$-specific $CD4^+$ T cells may have direct antitumor effects and augment $CD8^+$ T cell responses to self and/or mutated tumor antigens in patients with BRAF mutated cancers.

Introduction:

T cells can eliminate cancer cells through recognition of peptides from non-mutated or mutated proteins bound to cell surface MHC molecules(1). T cells specific for neoantigens derived from proteins encoded by mutated genes are increasingly recognized as important mediators of antitumor immunity in patients receiving checkpoint blocking antibodies(2-5) and adoptive T cell transfer(6, 7). Neoantigens are attractive targets for T cells because they are not subject to central and peripheral tolerance mechanisms that limit the frequency and function of T cells specific for self-antigens(8). Indeed, the burden of somatic mutations in multiple tumor types correlates with response to immune checkpoint inhibitors(4, 5, 9, 10), suggesting endogenous neoantigen-reactive T cells contribute to efficacy(11). Clinical response in patients with melanoma and cervical cancer treated with tumor infiltrating lymphocytes (TILs) has also correlated with the presence of neoantigen-reactive T cells in the administered TIL product(6, 11, 12). Most neoantigens are random, patient-specific, and heterogeneously expressed, which limits their broader utility as targets for adoptive transfer with engineered T cells in multiple patients with a particular tumor type(8). In contrast, driver mutations are actively selected, and expressed clonally and homogenously in cancers from many patients. Unfortunately, T cell responses to very few driver mutations have been described, perhaps as a consequence of selection based on HLA genotype(13).

The mutant BRAF kinase ($BRAF^{V600E}$) is an oncogenic driver present in 40% of melanoma, 10% of colorectal cancer, and 2% of lung cancer, and confers constitutive signaling that promotes tumor cell growth and survival. Small molecule BRAF inhibitors have impressive initial efficacy in melanoma, but resistance evolves by recruitment of alternative signaling pathways without loss of expression of $BRAF^{V600E}$ protein, suggesting that BRAF inhibitor-resistant melanoma would remain susceptible to T cells specific for the BRAF mutation(14). Here we describe a $CD4^+$ helper T cell response to $BRAF^{V600E}$ in a patient with an acral melanoma containing few nonsynonymous mutations who had a sustained complete response to TIL therapy.

Results and discussion

A 52-year-old man presented with stage IIIC, $BRAF^{V600E}$ mutated melanoma originating on the left foot and was treated with wide excision, completion lymph node dissection and adjuvant ipilimumab at 3mg/kg every 3 weeks for 4 doses, then every 3 months for maintenance. Before completing one year of ipilimumab, he relapsed with three in-transit metastases close to his left knee, which were resected. Three months later, he developed another in-transit metastasis at his left medial thigh, which was also resected. Three more months later, he progressed with a 3cm left iliac nodal metastasis and soft tissue nodular FDG-avid metastasis in the left thigh (Figure 1A). The iliac node was resected for whole exome sequencing and expansion of TIL, and the patient subsequently received TIL infusion following lymphodepleting chemotherapy. The left thigh lesion resolved and the patient remains free of disease 32 months after therapy.

Whole exome and RNA sequencing of purified tumor cells and normal tissue identified only 29 nonsynonymous missense mutations (Table S1) and no coding insertions or deletions, despite high mean coverage (over 100X for tumor and for normal) and adequate tumor purity as measured by the variant allele frequency of 35% of the often heterozygous BRAF V600E driver mutation. This result would be an unusually low number for sun-exposed melanoma, but is consistent with reported nonsynonymous mutation burden for other acral or mucosal tumors(15).

To identify potential neoantigen-reactive T cells that may have contributed to antitumor efficacy of TIL therapy, we stimulated peripheral blood mononuclear cells (PBMC) obtained from the patient after TIL therapy with a pool of overlapping peptides flanking each of the 20 mutations with the highest variant allele frequency and/or with evidence of RNA expression (Table S1). No $CD8^+$ T cell responses to candidate neoantigens were detected, however a $CD4^+$ T cell response specific for 20-mer peptides encompassing $BRAF^{V600E}$ was identified. The $BRAF^{V600E}$ reactive T cells were purified by IFN-γ capture and shown to recognize autologous B cells pulsed with mutant but not wildtype BRAF peptide, confirming specificity for the mutant peptide (Figure 1B). To determine whether $BRAF^{V600E}$ is processed and presented by class II MHC^+ APC, autologous B cells were transfected with mRNA encoding wildtype or mutant BRAF sequences targeted to the endosome. The T cells recognized B cells expressing mutant but not wildtype BRAF (Figure 1C). Recognition was blocked by anti-HLA-DQ but not anti-class I or anti HLA-DR identifying HLA-DQ as the likely restricting allele (Figure 1D). The patients class II MHC

haplotypes were HLA-DRB1*04 HLA-DQB1*0302/HLA-DRB1*09 HLA-DQB1*0303. Analysis of multiple B cell lines of known genotype suggested restriction by HLA-DQB1*03 paired with HLA-DQA1*03, with weak recognition of DQB1*0301 and stronger recognition of DQB1*0302 and DQB1*0303 (Table S2, Figure S1). B-LCL transfected with HLA-DQA1*0301 and DQB1*0302 cDNAs but not the HLA-DRB1*04 cDNA were recognized by $BRAF^{V600E}$-specific CD4 T cells when pulsed with the mutant peptide confirming the HLA restriction (Figure 1E). We tested recognition of three melanoma cell lines with an HLA-DQB1*0302 and $BRAF^{V600E}$ genotype. One tumor cell line that expressed the HLA-DQ and upregulated expression to interferon gamma was recognized by the $BRAF^{V600E}$-specific CD4 T cells suggesting the epitope can be presented directly by some tumor cells (Figure S2).

Tumor-specific $CD4^+$ T cells can have anti-tumor activity through direct cell killing and cytokine release(16, 17), but a major role is to support the development and function of $CD8^+$ T cells by licensing APC for efficient antigen presentation and producing cytokines(18, 19). Although we did not identify $CD8^+$ T cell responses to neoantigens in blood, these cells were the prevalent subset in TIL (Table S3). Moreover, a majority of IFN-γ produced by stimulation of multiple independent TIL cultures with autologous tumor was blocked by a HLA class I blocking antibody (Table S4). We evaluated TIL responses to neoantigens but did not observe IFN-γ production when TIL were cultured with autologous B cells pulsed with pools of peptides that included the 20 non-synonymous mutations screened previously (Figure 2A) or to autologous B cells transfected tandem RNA minigenes encoding the entire set of 29 potential nonsynonymous mutations (Figure S3). Any neoantigen-specific CD4 T cells present in the TIL product were below the level of detection of this assay. However, IFN-γ was produced after co-culture with B cells pulsed with peptides from lineage restricted self-antigens (tyrosinase, Mart-1, TRP2) and a cancer testes antigen (Mage A3), which are known targets of T cells in melanoma(20) (Figure 2B). Consistent with these results, CD8+ T cells in TIL produced IFN-γ in response to B cells transfected with minigenes encoding tyrosinase and Mart 1 (Figure S3). This data demonstrated that the patient's TIL contained $CD8^+$ T cell response to multiple self-antigens, but not to any of the putative neoantigens.

We utilized deep sequencing to identify TCR gene usage in $BRAF^{V600E}$-specific CD4+ T cells

and CD8 T cells. Three TCR Vb clonotypes showed marked expansion after stimulation of post-treatment PBMC with $BRAF^{V600E}$ peptide and these three sequences were further enriched after restimulation and IFN-γ capture (Figure 2C, table S5), suggesting each of these three clonotypes were specific for the BRAF V600E antigen. TCR Vb sequencing of tumor, TIL, and PBMC obtained prior to TIL infusion identified all 3 TCR Vb clones in the tumor, and 2 of 3 in TIL, albeit at relatively low frequency. All 3 TCR Vb sequences were below the level of detection in pre-treatment PBMC indicating enrichment at the tumor site (Figure 2D, Table S5). Analysis of TCR sequences in the TIL identified 34 Vb sequences that collectively made up >50% of the TIL product (Fig 2E, table S5). Only 5 of these 34 clones were detected in the blood prior to TIL infusion, with 4 at very low frequency (Fig 2F, table S5). We assessed TCR gene usage of the $CD8^+$ T cells that recognized each of the four lineage-specific or C/T antigens using IFN-γ capture to sort these cells from TIL. We identified 7 different Vb sequences that were highly enriched in the IFN-γ captured T cells, and these clonotypes represented 4.7% of the T cells in the TIL product (Figure S5, table S5). All 7 of these clonotypes and one of the BRAF-specific clonotypes were detected in blood obtained 10 and 24 months post TIL infusion demonstrating that TIL therapy resulted in sustained augmentation of T cell responses reacting with tumor antigens (Figure 2F,G, Tsble S5).

We next characterized the phenotype of circulating $BRAF^{V600E}$-specific CD4+ T cells from post-treatment blood samples using DQA1:0301/DQB1:0302 tetramers loaded with the mutant BRAF peptide (GDFGLATEKSRWSGS) for direct *ex vivo* staining, and isolate tetramer positive T cells for cloning. The specificity of the DQA1:0301/DQB1:0302/$BRAF^{V600E}$ tetramer was confirmed by showing that 24 out of 26 clones isolated by tetramer sorting released IFN-γ after re-challenging with the peptide. BRAF V600E-specific CD4 T cells showed an effector memory phenotype (CD45RA-CCR7-CD27-KLRG1+) and expressed low levels of PD-1 (Figure 3A). The majority of $BRAF^{V600E}$-specific cells expressed CXCR3 and CCR4. A fraction of the cells also expressed the skin-homing marker CLA. $BRAF^{V600E}$ peptide-activated cells produced IFN-γ, TNF-α, and IL-4, and IL-21 (Figure 3B), sometimes in combination (data not shown). Taken together, these data suggest that circulating BRAF-specific CD4 T cells after TIL infusion have a mixed Th1/Th2 phenotype, consistent with an established memory cellular immune response to mutated BRAF in melanoma.

Durable remissions in melanoma after adoptive transfer of self-antigen reactive $CD8^+$ T cells alone are exceedingly rare(21-23). The specificity of T cells responsible for tumor eradication after polyclonal TIL therapy is difficult to define precisely but it is tempting to speculate that the $BRAF^{V600E}$-specific $CD4^+$ T cells may have provided direct antitumor effects and aided the induction, persistence and function of self-antigen reactive $CD8^+$ T cells against a tumor that contained few neoantigens. The HLA-DQA1*03/DQB1*03 restricting allele for the $BRAF^{V600E}$-specific CD4 T cells is present in 29% of individuals in the International Histocompatibility Workgroup database(24), and isolation of the $BRAF^{V600E}$-specific TCR genes from this patient would facilitate adoptive therapy for patients with BRAF mutant tumors with TCR engineered T cells to test these hypotheses. TCR Va sequencing on samples with varying levels of BRAF reactive clones identified 4 TCR Va sequences that correlated in frequency with the three TCR Vb sequences (Figure 4A). A synthetic TCR comprising the dominant Va and Vb sequences was constructed and expressed in $CD4^+$ T cells from two healthy donors and conferred specificity to cells expressing $BRAF^{V600E}$ but not wildtype BRAF sequences (Figure 4B).

Immunotherapies that elicit or augment T cell responses to shared neoantigens derived from driver mutations are especially attractive because they allow treatment of multiple patients and should reduce antigen negative escape variants. Most studies have focused on neoantigen reactive $CD8^+$ T cells however recent work in murine models has highlighted the importance of local and systemic $CD4^+$ T cells in tumor rejection(25) (26). Indeed, the adoptive transfer of $CD4^+$ T cells specific for a non-driver neoantigen induced a clinical response in a single patient with cholangiocarcinoma (27). Although $BRAF^{V600E}$ is common in melanoma, and present in some thyroid, colon, and lung cancers, $CD8^+$ or $CD4^+$ T cells specific for this and other driver mutations are rarely identified(28, 29). One prior study isolated $BRAF^{V600E}$ specific $CD4^+$ T cells after repetitive peptide stimulation of PBMC, but a relationship to tumor localization or regression was not established(29). Our data identify $BRAF^{V600E}$-specific $CD4^+$ T cells restricted by a common class II MHC molecule enriched at the tumor site in a patient who achieved a durable remission after adoptive therapy with TIL and long-term persistence of $BRAF^{V600E}$-specific $CD4^+$ T cells and co-transferred $CD8^+$ T cells specific for self-antigens. The $BRAF^{V600E}$-specific TCR isolated in our study provides a reagent for future studies of adoptive cell therapy

with TCR transgenic $CD4^+$ T cells in patients with $BRAF^{V600E}$ positive tumors that express HLA-DQA1*03/DQB1*03, alone or in combination with $CD8^+$ T cells specific for self-antigens. This approach may determine the potential for direct antitumor effects and for augmenting $CD8^+$ T cell responses to other tumor associated antigens by targeting a driver mutation with $CD4^+$ T cells.

Methods:

The patient was enrolled under an FDA-approved IND and a clinical protocol approved by the Institutional Review Board of Fred Hutchinson Cancer Research Center (FHCRC 2643; NCT01807182).

ELISA assays were performed in technical duplicate or triplicate to allow qualitative measurement of large differences, and the mean of the technical replicates is presented in the figures along with the individual data points.

Author contributions:

J.R.V., S.L., M.F., I.C., T.S., W.K., and S.R.R. designed experiments, J.R.V, I.C., B.J., Y.Y.K., and J.K performed experiments, J.R.V., M.F., I.C., T.S., H.M.H., M.M., W.K., and S.R.R. analyzed the data, S.L, T. S. and J.A.T. provided materials, and J.R.V, S.L., M.F., I.C, J.A.T., W.K. and S.R.R. wrote the paper.

Acknowledgements:

J.R.V was supported by N.I.H grants T32 T32CA009515 and K12 CA076930-16A1 and a generous contribution from the Lembersky family. M.F. and J.R.V and S.R.R. were supported by a generous gift from the Bezos family. J.K was supported by the following grant EU-FP7-PEOPLE-2012-IOF 331255. M.M. was supported by N.I.H. grant 5U01CA176270-02. Thanks to Margot Pont for helpful advice on this project.

References Cited:

1. Restifo NP, Dudley ME, and Rosenberg SA. Adoptive immunotherapy for cancer: harnessing the T cell response. *Nature reviews Immunology.* 2012;12(4):269.
2. Gubin MM, Zhang X, Schuster H, Caron E, Ward JP, Noguchi T, Ivanova Y, Hundal J, Arthur CD, and Krebber W-J. Checkpoint blockade cancer immunotherapy targets tumour-specific mutant antigens. *Nature.* 2014;515(7528):577-81.

3. McGranahan N, Furness AJS, Rosenthal R, Ramskov S, Lyngaa R, Saini SK, Jamal-Hanjani M, Wilson GA, Birkbak NJ, Hiley CT, et al. Clonal neoantigens elicit T cell immunoreactivity and sensitivity to immune checkpoint blockade. *Science.* 2016.
4. Rizvi NA, Hellmann MD, Snyder A, Kvistborg P, Makarov V, Havel JJ, Lee W, Yuan J, Wong P, Ho TS, et al. Cancer immunology. Mutational landscape determines sensitivity to PD-1 blockade in non-small cell lung cancer. *Science.* 2015;348(6230):124-8.
5. Le DT, Durham JN, Smith KN, Wang H, Bartlett BR, Aulakh LK, Lu S, Kemberling H, Wilt C, and Luber BS. Mismatch-repair deficiency predicts response of solid tumors to PD-1 blockade. *Science.* 2017:eaan6733.
6. Lu Y-C, Yao X, Crystal JS, Li YF, El-Gamil M, Gross C, Davis L, Dudley ME, Yang JC, and Samuels Y. Efficient identification of mutated cancer antigens recognized by T cells associated with durable tumor regressions. *Clinical Cancer Research.* 2014;20(13):3401-10.
7. Lennerz V, Fatho M, Gentilini C, Frye RA, Lifke A, Ferel D, Wölfel C, Huber C, and Wölfel T. The response of autologous T cells to a human melanoma is dominated by mutated neoantigens. *Proceedings of the National Academy of Sciences of the United States of America.* 2005;102(44):16013-8.
8. Schumacher TN, and Schreiber RD. Neoantigens in cancer immunotherapy. *Science.* 2015;348(6230):69-74.
9. Snyder A, Makarov V, Merghoub T, Yuan J, Zaretsky JM, Desrichard A, Walsh LA, Postow MA, Wong P, and Ho TS. Genetic basis for clinical response to CTLA-4 blockade in melanoma. *New England Journal of Medicine.* 2014;371(23):2189-99.
10. Le DT, Uram JN, Wang H, Bartlett BR, Kemberling H, Eyring AD, Skora AD, Luber BS, Azad NS, and Laheru D. PD-1 blockade in tumors with mismatch-repair deficiency. *New England Journal of Medicine.* 2015;372(26):2509-20.
11. Tran E, Robbins PF, and Rosenberg SA. 'Final common pathway'of human cancer immunotherapy: targeting random somatic mutations. *Nature Immunology.* 2017;18(3):255-62.
12. Rosenberg SA, and Restifo NP. Adoptive cell transfer as personalized immunotherapy for human cancer. *Science.* 2015;348(6230):62-8.
13. Marty R, Kaabinejadian S, Rossell D, Slifker MJ, van de Haar J, Engin HB, de Prisco N, Ideker T, Hildebrand WH, and Font-Burgada J. MHC-I Genotype Restricts the Oncogenic Mutational Landscape. *Cell.* 2017.
14. Shi H, Hugo W, Kong X, Hong A, Koya RC, Moriceau G, Chodon T, Guo R, Johnson DB, and Dahlman KB. Acquired resistance and clonal evolution in melanoma during BRAF inhibitor therapy. *Cancer discovery.* 2014;4(1):80-93.
15. Krauthammer M, Kong Y, Ha BH, Evans P, Bacchiocchi A, McCusker JP, Cheng E, Davis MJ, Goh G, and Choi M. Exome sequencing identifies recurrent somatic RAC1 mutations in melanoma. *Nature genetics.* 2012;44(9):1006-14.
16. Quezada SA, Simpson TR, Peggs KS, Merghoub T, Vider J, Fan X, Blasberg R, Yagita H, Muranski P, and Antony PA. Tumor-reactive CD4+ T cells develop cytotoxic activity and eradicate large established melanoma after transfer into lymphopenic hosts. *Journal of Experimental Medicine.* 2010;207(3):637-50.

17. Manici S, Sturniolo T, Imro MA, Hammer J, Sinigaglia F, Noppen C, Spagnoli G, Mazzi B, Bellone M, and Dellabona P. Melanoma cells present a MAGE-3 epitope to CD4+ cytotoxic T cells in association with histocompatibility leukocyte antigen DR11. *Journal of Experimental Medicine.* 1999;189(5):871-6.
18. Sun JC, and Bevan MJ. Defective CD8 T cell memory following acute infection without CD4 T cell help. *Science.* 2003;300(5617):339-42.
19. Williams MA, Tyznik AJ, and Bevan MJ. Interleukin-2 signals during priming are required for secondary expansion of CD8+ memory T cells. *nature.* 2006;441(7095):890-3.
20. Gros A, Parkhurst MR, Tran E, Pasetto A, Robbins PF, Ilyas S, Prickett TD, Gartner JJ, Crystal JS, and Roberts IM. Prospective identification of neoantigen-specific lymphocytes in the peripheral blood of melanoma patients. *Nature Medicine.* 2016.
21. Johnson LA, Morgan RA, Dudley ME, Cassard L, Yang JC, Hughes MS, Kammula US, Royal RE, Sherry RM, and Wunderlich JR. Gene therapy with human and mouse T-cell receptors mediates cancer regression and targets normal tissues expressing cognate antigen. *Blood.* 2009;114(3):535-46.
22. Yee C, Thompson JA, Byrd D, Riddell SR, Roche P, Celis E, and Greenberg PD. Adoptive T cell therapy using antigen-specific CD8+ T cell clones for the treatment of patients with metastatic melanoma: in vivo persistence, migration, and antitumor effect of transferred T cells. *Proceedings of the National Academy of Sciences.* 2002;99(25):16168-73.
23. Dudley ME, Wunderlich J, Nishimura MI, Yu D, Yang JC, Topalian SL, Schwartzentruber DJ, Hwu P, Marincola FM, and Sherry R. Adoptive transfer of cloned melanoma-reactive T lymphocytes for the treatment of patients with metastatic melanoma. *Journal of immunotherapy.* 2001;24(4):363-73.
24. Petersdorf E. 2017.
25. Spitzer MH, Carmi Y, Reticker-Flynn NE, Kwek SS, Madhireddy D, Martins MM, Gherardini PF, Prestwood TR, Chabon J, and Bendall SC. Systemic Immunity Is Required for Effective Cancer Immunotherapy. *Cell.* 2017;168(3):487-502. e15.
26. Kreiter S, Vormehr M, Van de Roemer N, Diken M, Löwer M, Diekmann J, Boegel S, Schrörs B, Vascotto F, and Castle JC. Mutant MHC class II epitopes drive therapeutic immune responses to cancer. *Nature.* 2015;520(7549):692-6.
27. Tran E, Turcotte S, Gros A, Robbins PF, Lu Y-C, Dudley ME, Wunderlich JR, Somerville RP, Hogan K, and Hinrichs CS. Cancer immunotherapy based on mutation-specific CD4+ T cells in a patient with epithelial cancer. *Science.* 2014;344(6184):641-5.
28. Tran E, Robbins PF, Lu Y-C, Prickett TD, Gartner JJ, Jia L, Pasetto A, Zheng Z, Ray S, and Groh EM. T-Cell Transfer Therapy Targeting Mutant KRAS in Cancer. *New England Journal of Medicine.* 2016;375(23):2255-62.
29. Sharkey MS, Lizée G, Gonzales MI, Patel S, and Topalian SL. CD4+ T-cell recognition of mutated B-RAF in melanoma patients harboring the V599E mutation. *Cancer research.* 2004;64(5):1595-9.

Figures:

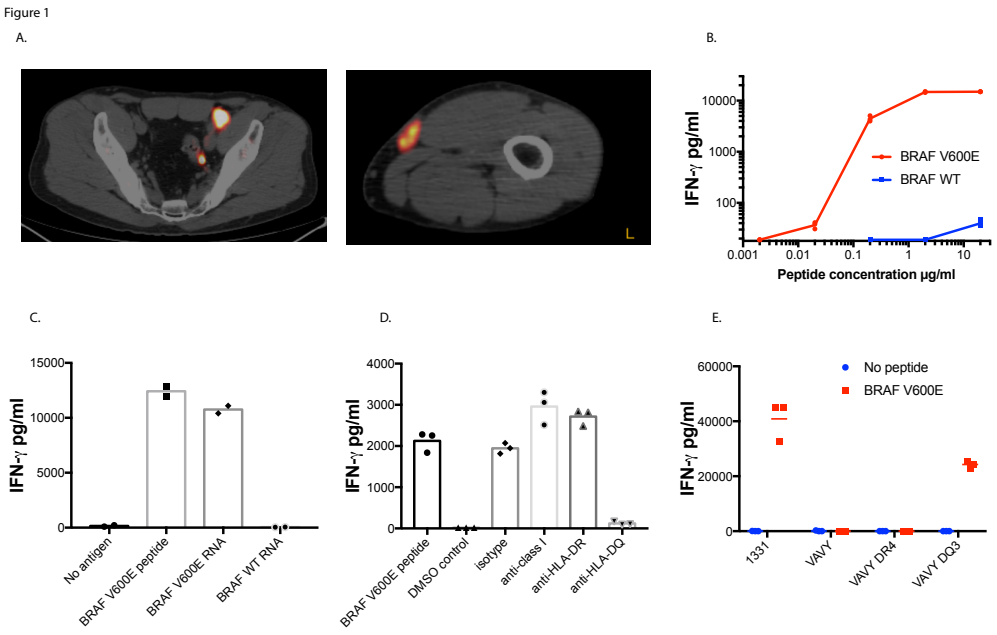

Figure 1.

CD4^{+} T cells specific for BRAF^{V600E} isolated from post TIL infusion PBMC are restricted by HLA DQB1 03

A). Positron emission tomography showing recurrent tumor in left iliac region (left) and left thigh (right). B-D) Specificity and HLA restriction of BRAF^{V600E}-specific T cells. B) IFN-γ production by a patient-derived T cell line incubated with autologous B cells pulsed with wildtype and mutant BRAF peptide. C) Recognition of autologous B cells transfected with mRNA encoding mutant or wildtype BRAF sequences. D) Recognition of autologous B cells pulsed with mutated BRAF peptide in the presence or absence of HLA blocking antibodies. E) BRAF-specific CD4^{+} T cells recognition of the B-LCL line 1331 (DR0404, DQA1*0301/DQB1*0302) which is matched at HLA-DQ with the patient, and the HLA-DQ mismatched B-LCL line VAVY (DR3, DQA1*0501/DQB1*0201) prior to and after transduction with HLA-DRB1*0404 (DR4) or HLA-DQB1*0302/DQA1*0301 (DQ8). Assays were performed with and without pulsing with BRAF^{V600E} peptide. Experiments were performed with 2-3 technical replicates.

Figure 2

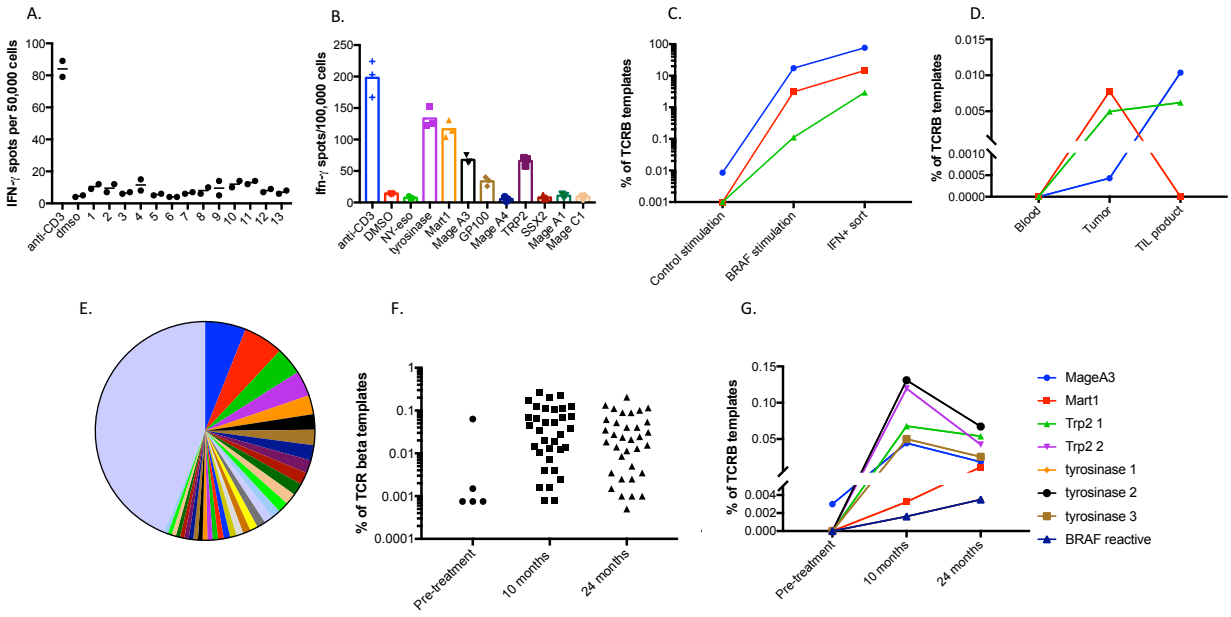

Figure 2.

Specificity of CD8^{+} T cells in TIL and TCR sequencing of T cell clonotypes in blood after adoptive transfer

TIL were incubated with autologous B cells pulsed with peptide pools encompassing tumor associated antigens from mutated antigens (A) and tumor associated self-antigens (B) and IFN-γ release was measured by elispot with 2-3 technical replicates. C) Frequency of TCRVb sequences in peripheral blood mononuclear cells after mock stimulation, BRAF^{V600E} peptide stimulation, or after sorting IFN-γ secreting cells after BRAF^{V600E} peptide restimulation. CDR3 sequences: CASNEGNSGNTIYF (blue), CASGARQIPYTF(red), CASSLSAAGGGYGYTF (green) D) TCRVb clonotypes of BRAF-specific T cells were quantitated by TCRB sequencing of pre-treatment blood, tumor single cell suspension, and the TIL product infused into the patient. E) TCRVb sequences in TIL product ranked by prevalence, with the top 34 clones in colors and the remainder in grey F) Frequency of the top 34 TIL TCR Vb clonotypes from D in pretreatment blood and post-treatment blood obtained at 10 and 24 months. G) Frequency of TCR Vb clonotypes of CD4^{+} BRAF^{V600E} and CD8^{+} T cells specific for the specified antigens in pretreatment and post-treatment blood.

Figure 3

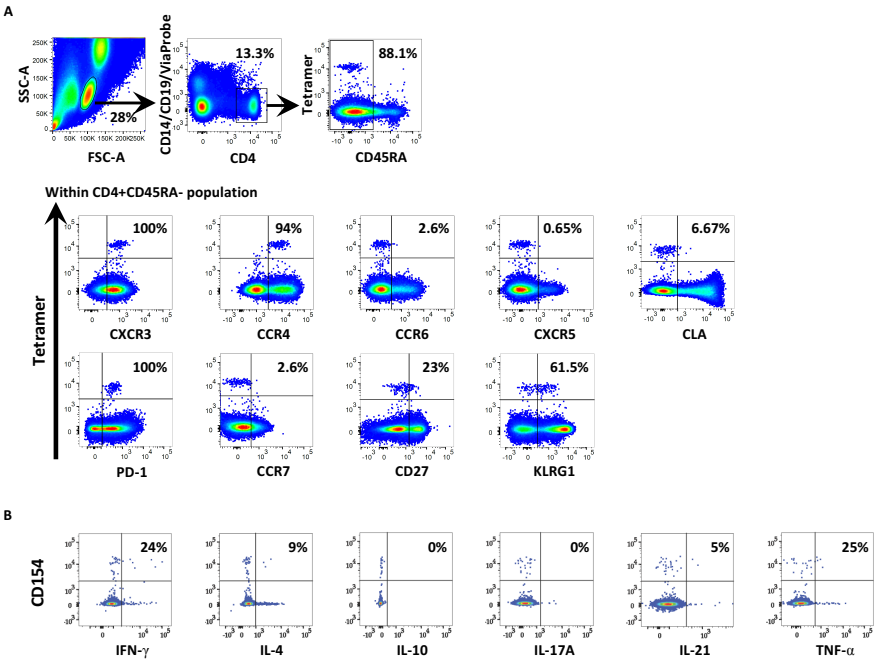

Figure 3.

Phenotypic analysis for BRAF-specific T cells following TIL treatment.

In (A), a dump channel was used to exclude monocytes (CD14+), B cells (CD19+), and dead cells (ViaProbe) from lymphocytes. Viable CD4+ T cells were plotted against tetramer and CD45RA. CD45RA negative memory cells (88.1% of CD4) that were tetramer positive and negative were next plotted against surface markers indicated in the figure. Numbers indicate the percentage of cells in the gated regions or the percentage of tetramer-positive cells for each marker. In (B), intracellular cytokine staining revealed that activated (CD154+) BRAF-specific T cells secreted IFN-γ, IL-4, TNF-α, and IL-21.

Figure 4

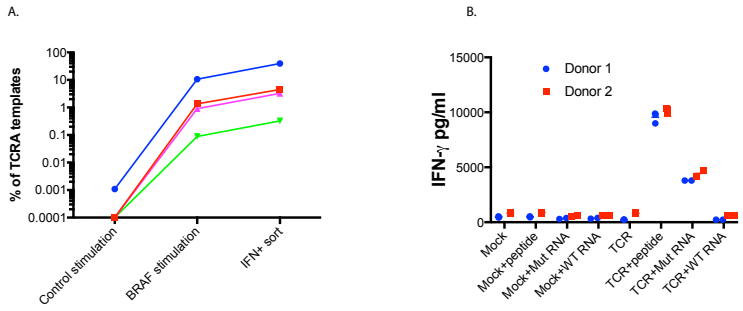

Figure 4.

A synthetic TCR derived from the dominant Va and Vb sequences recognizes cells expressing BRAFV600E

A) Frequency of TCRBVa sequences in peripheral blood mononuclear cells after mock stimulation, BRAF V600E stimulation, or after sorting IFN-γ secretion cells after BRAF V600E peptide restimutation. CDR3 sequences: CAVRRGNNDMRF (blue), CIVRAYSGYSTLTF (red), CAVITLNNNAGNMLTF (purple), CAVTSNAGKSTF (green). B) IFN-γ production by CD4+ T cells from two normal donors transduced with a synthetic TCR construct and incubated with an HLA-DQB1*0302 B cell line 1331 pulsed with BRAF V600E peptide or transfected with mRNA encoding mutant or wildtype BRAF sequences with 2 technical replicates.

Supplemental Materials and methods:

Clinical protocol:

The patient was enrolled for TIL generation under an FDA-approved IND and a clinical protocol approved by the Institutional Review Board of Fred Hutchinson Cancer Research Center (FHCRC 2643; NCT01807182). Patients with stage IV melanoma, or stage III unlikely to be cured by surgery, >18 years of age, with an ECOG </=1, with a site of metastatic disease that could be safely resected or biopsied, were eligible. TIL were expanded from tumor fragments in 6,000 IU/ml recombinant IL-2 (Proleukin; Novartis), using methodologies developed at the Surgery Branch of the National Cancer Institute{Dudley, 2001 #101}. TIL cultures were selected based on cell growth and autologous tumor reactivity as determined by IFN–γ secretion after co-culture with autologous tumor cells. The TIL were cryopreserved until needed for use, then thawed and further expanded using a rapid expansion protocol, as previously-described{Riddell, 1990 #126}. The expanded TIL were administered to the patient following a lymphodepleting chemotherapy regimen of cyclophosphamide 60mg/kg/day x 2 days, then fludarabine 25 mg/m^2/day x 5 days. Within 24 hours of the TIL infusion, the patient received high-dose IL-2 at 600,000 IU/kg IV every 8 hours, for a total of 9 doses. Tumor responses were assessed using RECIST version 1.1 with CT and MRI at weeks 6, 12, and 24, then every 3-6 months, at the discretion of the primary provider.

T cell culture:

Initial stimulations were performed with overlapping 20-mer crude peptides obtained from Elim Biopharma, with 2 peptides spanning each mutation with the mutated residue at position +7 or +13 of the 20 amino acid sequence. Subsequent experiments were performed with >80% purity 21 mer peptides with V600 (wildtype) or E600 (mutant) at position +11. Cryopreserved PBMC were thawed and rested overnight in CTL (RPMI media with L-glutamine and HEPES (Gibco) supplemented with 10% human serum (produced in house), 50 μM beta-mercaptoethanol, penicillin and streptomycin, 4 mM L-glutamine and 2ng/ml recombinant human IL-7 (Peprotech). The following morning PBMC were washed and stimulated at 10e6 cells in 5 ml CTL per well of a 6 well plate with a pool of 1μg/ml of each peptide without cytokines. Recombinant IL-2 (Peprotech) was added to a final concentration of 10 U/ml on day

+3, and half media changes with supplemental IL-2 were performed on days +3, +6, and +9. On day +13 cells were used in an ELISA and cytokine staining assays. Antigen specific T cell enrichment was carried out by staining live cells for secreted IFN-γ using the IFN-γ secretion assay APC (Milltenyi) following the manufacturer's instructions, and using autologous B cells as antigen presenting cells pulsed with 10 μg/ml 21-mer BRAF mutant peptide. $CD4^+$ IFN-γ secreting cells were sorted on a FACS Aria2. Sorted cells were rested in CTL supplemented with 10 ng/ml human IL-15 for 5 days, then expanded using a rapid expansion protocol described previously{Riddell, 1990 #126}. Antigen-specific T cells were further enriched by sorting for Vbeta3.1 positive, $CD4^+$ cells by staining with anti-Vbeta 3.1 (Thermo Scientific, cat TCR2740), expanded, and cryopreserved at day 13 or 14 after expansion. Cryopreserved cells were thawed and rested overnight in CTL supplemented with 10 U/ml IL-2 prior to assays.

Antigen presenting cells

Autologous B cells were isolated from fresh or thawed PBMC using magnetic beads coated with antibodies recognizing CD19 (Miltenyi, cat 130-050-301) and magnetic positive selection according to the manufacturer's instructions (Miltenyi, cat 13 for 7 days in B cell medium supplemented with 200U/ml human IL-4 (Peprotech) as described {Tran, 2014 #45}. B cells were subsequently harvested and restimulated with 3T3 CD40L and fresh medium every 3 days. B cells were used in assays at day +3 of stimulation 2 or 3.

Phenotyping of tumor infiltrating lymphocytes

Cells were thawed, washed, and counted using Trypan blue and pre-incubated with Fc receptor blocking solution (Biolegend) to reduce non-specific binding and subsequently stained in two panels with fluorochrome-conjugated anti-human antibodies against CD45, CD3, CD4, CD8, CD56, gdTCR, CD25, CD127, CCR7, CD45RA, PD1 and TIM3 for 30 min on ice, washed and stained with fixable viability dye (FVD, eBioscience), before fixation (IC fixation buffer, eBioscience). Intracellular cytokine expression was measured using flow cytometry. Cells were cultured in RPMI-1640 with 10% FBS, 1% Pen/Strep, 50ngml 1 PMA, 1mgml 1 ionomycin for 5h at 37°C with 5% CO2. GolgiStop (monensin) was added for the last 2 h. Following stimulation, cells were washed, resuspended and stained with FVD. Subsequently, cells were fixed and permeabilized using a BD Cytofix/Cytoperm kit and stained for 30 min at 4 °C with

fluorochrome-conjugated antibodies against CD45, CD3, CD4, CD8, gdTCR, IFNg, IL-17A and IL-22.

mRNA transfection

RNA expression targeted to the endosome was carried out using the method described by the Sahin group{Kreiter, 2008 #124} where antigens are targeted to the endosome by fusion of the antigen to class I MHC sorting signals. The mRNA expression construct pJV57 was constructed by gene synthesis (Geneart, Life Sciences), which contained a T7 promoter fused to the N terminal 25 amino acids of the human HLA-B gene, followed by a BamHI restriction site, the coding sequence of enhanced GFP, an AgeI restriction site, the C terminal 55 amino acids of the human HLA-B gene, followed by the human beta globin untranslated region followed by a 30 nucleotide poly A tail followed by a SapI restriction site directing cleavage in the poly A tail. pJV84 was cloned by ligating the following into AgeI/BamHI digested pJV57: annealed oligonucleotides (Ultramers, Integrated DNA Technologies) encoding BRAF amino acids 575-624 flanked by a 5' AgeI and 3' BamHI site containing the E600 substitution. pJV85 was made by ligating annealed oligonucleotides (Ultramers, Integrated DNA Technologies) encoding BRAF amino acids 575-624 flanked by a 5' AgeI and 3' BamHI site containing the wildtype V600 amino acid.

3 tandem minigenes encoding 27-mer peptide sequences for 10, 10 and 9 (29 total) mutations or the coding sequences of tyrosinase, SSX2, MageA3, Mart1 and GP100 were codon optimized, constructed by gene synthesis (Geneart, Life Sciences) and cloned into the AgeI/BamHI sites of JV57.

pJV84 and pJV85 and other plasmids based on JV57 were linearized with SapI (Thermo Fisher) and mRNA was in vitro transcribed using the Highscribe T7 ARCA mRNA kit (New England Biolabs) and purified by lithium precipitation according to the manufacturer's instructions. mRNA was electroporated into CD40L stimulated B cells 16 hours prior to co-culture experiments as described {Tran, 2014 #45}.

Cytokine release assays

In ELISA assays, 50,000 effector T cells were incubated in 96 well round bottom plates with 100,000 B cells or B-LCL lines and 10 μg/ml or specific concentrations of peptides in RPMI

(Gibco) supplemented with 5% heat inactivated fetal bovine serum. IFN-γ in supernatants was quantitated using the ready set go human IFN-γ ELISA kit (eBioscience) in technical triplicate. HLA blocking experiments were carried out with 20 μg/ml antibody anti class I (Biolegend, cat 311411) anti HLA DR (clone L243, cat 307611) and HLA-DQ (Abcam, clone spv-l3, cat. ab23632) added 1 hour prior to adding peptide. For elispot assays, 50,000 tumor infiltrating lymphocytes were incubated with 200,000 autologous B cells pulsed with peptide pools at a final concentration of 10 μg/ml of each peptide in CTL medium using the human IFN-γ ELISpot-Pro kit (Mabtech) and developed using the manufacturer's instructions.

TCR Vb and Va sequencing:

DNA from clinical samples were isolated using the Qiagen DNeasy or Qiamp micro DNA kits according to the manufacturer's instructions. TCRB sequencing was carried out using the human TCRB sequencing kit (Adaptive Biotechnology) following the manufacturer's instructions and sequenced using a MiSeq (Fred Hutchinson Cancer Research Center Genomics core) with data analysis carried out by Adaptive biotechnology software. TCRA sequencing was carried out using the human TCRA sequencing service (Adaptive Biotechnology).

HLA identification

LCL cell lines 1331, DUCAF, VAVY, BM14, DEM and DEU were obtained from the research cell bank (Seattle, WA). The remainder of the cell lines were a generous gift from Marie Bleakley, Fred Hutchinson Cancer Research Center. For coculture assays, LCL cell lines were pulsed with 10 μg/ml of BRAF mutant peptide or DMSO control for 4 hours and then washed 3 times with PBS prior to ELISA assay. For identification of specific class II alleles, codon optimized linear DNA fragments encoding HLA-DRB1 0404 protein or the HLA-DQB1 0302 protein linked by a T2A skip sequence to HLA-DQA1 0301 protein were synthesized genestrings (Life Sciences). and cloned into the vector MP71{Engels, 2003 #104} linearized with NotI and EcoRI (Thermo Fisher) using the NEBuilder cloning kit (New England Biolabs) and sequence verified. Retroviral transduction was performed as described{Sommermeyer, 2015 #105} into the VAVY cell line homozygous for HLA DRB1 0301 DQA1 0501 and DQB1 0201 (Research cell bank). Cells positive for DRB1 0404 were sorted on a FACSAria2 sorter using the antibody DRB1-PE (Biolegend, cat 362303) and cells positive for DQB1 03 DQA1 03 were

sorted using the anti DQ antibody clone HLADQ1-FITC (Biolegend, cat 318104).

T cell receptor construction

TCR construction was in the vector PRRL{Jones, 2009 #118} further modified by introducing six point mutations into the start codon and putative promoter region of the woodchuck hepatitis virus X protein as in {Lim, 2016 #119} with the beta chain followed by a P2A translational skip sequence followed by the alpha chain with cysteines introduced to facilitate pairing{Kuball, 2007 #120}. A codon optimized DNA fragment containing the TRBV28 and CDR3 and TRBJ1-3 sequences followed by TCRB1 sequence with a cysteine substituted at residue 57 followed by a P2A skip sequence and the TRAV21 and CDR3 sequences followed by TRAJ43 and TRAC sequences was synthesized as a genestring (Life Sciences) and cloned using the NEBuilder cloning kit (New England Biolabs) into the vector PRRL-SIN linearized with PstI and AscI (Thermo Fisher) and sequence verified. One week after transduction, cells were sorted based on Vbeta3.1 expression using antibody clone 8F10 (Thermo Scientific, cat TCR2740) and expanded via rapid expansion as described above. T cells were used in assays or cryopreserved on day 14 of the rapid expansion.

Nucleic acid preparation for exome capture and RNA sequencing:

Post-treatment blood was used to isolate non-tumor DNA. A single-cell suspension derived from the iliac nodal tumor recurrence was flow sorted (propidium iodide negative and CD45 negative) to deplete abundant infiltrating lymphocytes and enrich for neoplastic cells. Normal tissue and sorted tumor cells were processed with the Qiagen DNA/RNA AllPrep Micro kit to isolate DNA for exome capture, with RNA reserved for subsequent RNA-seq profiling. Genomic DNA concentration was quantified on an Invitrogen Qubit® 2.0 Fluorometer (Life Technologies-Invitrogen, Carlsbad, CA, USA) and Trinean DropSense96 spectrophotometer (Caliper Life Sciences, Hopkinton, MA).

HLA typing:

High resolution HLA typing was carried out by the CLIA approved clinical HLA typing laboratory at the Fred Hutchinson Cancer Research Center.

Whole exome sequencing:

Exome sequencing libraries were prepared using the Agilent SureSelectXT Reagent Kit and exon targets isolated using the Agilent All Human Exon v6 (Agilent Technologies, Santa Clara, CA, USA). 200 ng of genomic DNA was fragmented using a Covaris LE220 focused-ultrasonicator (Covaris, Inc., Woburn, MA, USA) and libraries prepared and captured on a Sciclone NGSx Workstation (PerkinElmer, Waltham, MA, USA). Library size distributions were validated using an Agilent 2200 TapeStation. Additional library QC, blending of pooled indexed libraries, and cluster optimization was performed using Life Technologies' Invitrogen Qubit® 2.0 Fluorometer.

The resulting libraries were sequenced on an Illumina HiSeq 2500 using a paired-end 100bp (PE100) strategy. Image analysis and base calling was performed using Illumina's Real Time Analysis v1.18 software, followed by "demultiplexing" of indexed reads and generation of FASTQ files using Illumina's bcl2fastq Conversion Software v1.8.4 (http://support.illumina.com/downloads/bcl2fastq_conversion_software_184.html). Read pairs passing standard Illumina quality filters were retained for further analysis, yielding 77M read pairs for the tumor and 89M read pairs for the normal. Paired reads were aligned to the human genome reference (GRCh37/hg19) with the BWA-MEM short-read aligner{Li, 2013 #110;Li, 2009 #111}. The resulting alignment files, in standard BAM format, were processed by Picard 2.0.1 and GATK 3.5{McKenna, 2010 #109} for quality score recalibration, indel realignment, and duplicate removal according to recommended best practices{Auwera, 2013 #116}.

The resulting alignments were checked for quality and consistency using several tools. The GATK DepthOfCoverage tool confirmed that mean coverage of the 60MB capture region is 107X and 125X for the tumor and normal WES alignments respectively. The GATK DiagnoseTargets command determined that 97% of the capture regions were of sufficient quality to call variants (ie. were not LOW_COVERAGE, POOR_QUALITY, etc.). We next used ConPair{Bergmann, 2016 #127} to verify that the tumor and normal were correctly paired and that there was minimal cross-contamination between the two. Conpair confirmed that the two samples are from the same individual (concordance 0.99) and that both the tumor and normal sample contamination levels are less than 0.1%.

To call somatic mutations from the analysis-ready tumor and normal BAM files, we used three independent software packages: MuTect 1.1.7{Cibulskis, 2013 #114}, Strelka 1.0.14{Saunders, 2012 #117}, and VarScan.v2.4.1{Koboldt, 2012 #113}. Variant calls from all tools, in VCF format, were annotated with Oncotator{Ramos, 2015 #108}. Annotated missense somatic variants were combined into a single summary as follows. First, any mutation annotated as "somatic" but present in dbSNP was removed if it was not also present in COSMIC or its minor allele frequency was greater than 1% (according to the UCSC Genome Browser snp150Common table). Variants supported by two or more variant callers were retained and those supported by only one variant caller were subject to manual inspection.

In addition to single-base changes in code, three potential splice-site mutations were identified by two or more variant callers. Inspection of RNA-seq data near these sites showed no evidence of discernible effect on splicing, so these three mutations were excluded from further consideration. VarScan and Strelka are capable of detecting somatic insertions and deletions as well, but the two callers reported only two frameshift deletions in common. On inspection both were found to be likely alignment errors also present in the normal sample.

RNA-Seq data processing:

To rank candidate peptides by observed expression level, we also performed RNA-seq on flow-sorted tumor cells from the same single cell suspension. RNA-seq libraries were prepared from total RNA using the TruSeq RNA Sample Prep v2 Kit (Illumina, Inc., San Diego, CA, USA) and a Sciclone NGSx Workstation (PerkinElmer, Waltham, MA, USA). Library size distributions were validated using an Agilent 2200 TapeStation (Agilent Technologies, Santa Clara, CA, USA). Additional library QC, blending of pooled indexed libraries, and cluster optimization was performed using Life Technologies' Invitrogen Qubit® 2.0 Fluorometer (Life Technologies-Invitrogen, Carlsbad, CA, USA). The library was sequenced on an Illumina HiSeq 2500 to generate 133M 50nt paired reads (PE50). Reads were aligned to a RefSeq derived reference transcriptome with RSEM 1.2.19{Li, 2011 #112}. Gene-level expression values from RSEM, in TPM units, were added to our summary of missense somatic variants.

DQ proteins and tetramers

Recombinant DQ8 (DQA1:0301/DQB1:0302) proteins were produced as previously described{Chow, 2014 #128}. Briefly, soluble DQ proteins were purified from insect cell culture supernatants by affinity chromatography. For the preparation of HLA class II tetramers, DQ proteins were in vivo biotinylated in Drosophila S2 cells prior to harvest and exchanged to citric/phosphate buffer, pH 5.4. The biotinylated monomer was loaded with 0.2 mg/ml of peptide by incubating at 37°C for 72 h in the presence of 0.2 mg/ml n-Dodecyl-β-maltoside and 1 mM Pefabloc SC (Sigma–Aldrich, St. Louis, MO). Peptide loaded monomers were subsequently conjugated into tetramers using R-PE streptavidin (Biosource International, Camarillo, CA) at a molar ratio of 8:1.

T cell clone isolation

BRAF-specific T cell clones were generated by performing single-cell sort on tetramer-positive CD4+ cells from direct *ex vivo* staining using a FACSAria II. Clones were expanded in a 96-well plate in the presence of 1.0 x 10^5 irradiated PBMCs, 2 μg/ml phytohemagglutinin (Remel Inc. Lenexa, KS), and IL-2 (10U/ml). After expansion of each T cell clone into a single 48 well, clones were incubated with autologous B cells pulsed with the 15-mer BRAF V600E peptide and IFN-γ production was measured by ELISA.

HLA-DQ8/BRAF tetramer enrichment and analysis

Ex vivo HLA-DQ8/BRAF tetramer staining and enrichment was done as previously described (*Int Immunol* 25(8): 447–457, 2014). 30-40 million PBMC were thawed and rested overnight at room temperature. Tetramer staining was performed in the 5ml polystyrene FACS tubes (BD Biosciences, San Jose, CA, USA) at 150-200 million PBMC/ml in 200 µl T-cell culture medium (RPMI 1640 (GIBCO, Life Technologies, Carlsbad, CA, USA) with 10% in-house pooled human serum and 1% Penicillin Streptomycin (GIBCO, Life Technologies, Carlsbad, CA, USA)). 6µl of tetramer was added to the cell suspension and incubated at room temperature for 2 hours. After tetramer staining, cells were incubated with 40µl anti-PE magnetic beads and enriched using magnetic columns based on manufacturer's instructions (Miltenyi Biotec, Auburn, CA, USA). Before enrichment, 1/100th cell fraction was set aside for antibody staining ('Pre'). All fluorescent antibodies were obtained from BioLegend (San Diego, CA, USA) unless otherwise stated. Enriched samples were stained with fluorecent antibody cocktail containing

anti-CXCR3 FITC (clone G025H7), anti-CD14 PerCP Cy5.5 (clone 61D3) (eBioscience, Waltham, MA, USA), anti-CD19 PerCP Cy5.5 (clone SJ25C1) (eBioscience, Waltham, MA, USA), anti-PD-1 PECy7 (clone EH12.2H7), anti-KLRG1 APC (clone SA231A2), anti-CCR7 APCCy7 (clone G043H7), anti-CD45RA Alexa Fluor® 700 (clone HI100), anti-CCR6 BV421 (clone G034E3), anti-CCR4 BV510 (clone L291H4), CLA-BV605 (clone HECA-452) (BD Biosciences, San Jose, CA, USA), anti-CD27 BV650 (clone 0323) and anti-CD4 BUV737 (clone SK3) (BD Biosciences, San Jose, CA, USA). Both 'Pre' and enriched samples were incubated at room temperature for 20 minutes. ViaProbe (Miltenyi Biotec, Auburn, CA, USA) was added to the samples before analysing on the flow cytometer, BD FACSAria Fusion (BD Biosciences, San Jose, CA, USA). CD14, CD19 and ViaProbe were used to exclude monocytes, B-cells and dead cells from post-acquisition analysis. Sample analysis was done with FlowJo, LLC (BD Biosciences, San Jose, CA, USA).

Intracellular cytokine staining

PBMC from post-treatment melanoma patients were resuspended in T cell medium at a concentration of 5 million/mL. Cells were stimulated with 1 μl of 20 mg/mL BRAF V660E peptide (GDFGLATEKSRWSGS) for 7 hours. Golgistop (BD Biosciences) was added to the culture at 1:1500 dilution 3 hours before harvest. After incubation, cells were stained with anti-CD154 PE (clone 5C8, Miltenyi Biotec) at room temperature for 10 min, followed by incubation with anti-PE bead at 4^{o}C for an additional 10 min (Miltenyi Biotec). CD154+ cells were enriched using magnetic columns based on manufacturer's instructions (Miltenyi Biotec). Enriched cells were stained with surface antibodies including anti-CD4 BV650 (clone SK3, BioLegend), anti-CD14 Pacific Blue (clone M5E2, BioLegend). Anti-CD19 Pacific Blue (clone HIB19, BioLegend), anti-CD45RA BV510 (clone HI100, BD Biosciences) as well as Fixable Viability Stain 450 (BD Horizon). After surface staining, cells were fixed and permeabilized as per the manufacturer's instructions (eBioscience). Cells were next stained with antibodies against IFN-γ Alexa Fluor® 700 (clone 4S.B3, BioLegend), IL-4 FITC (clone 8D4-8, eBioscience), IL-10 PE/Cy7 (clone JES3-9D7, BioLegend), IL-17A APC/Cy7 (clone BL168, BioLegend), IL-21 APC (clone eBio3A3-N2. eBioscience), and TNF-α (clone MAb11, eBioscience) for 20 minutes at room temperature. Cells were washed and immediately analyzed on a BD LSRFortessa multi-color flow cytometer.

1. Dudley ME, Wunderlich J, Nishimura MI, Yu D, Yang JC, Topalian SL, Schwartzentruber DJ, Hwu P, Marincola FM, and Sherry R. Adoptive transfer of cloned melanoma-reactive T lymphocytes for the treatment of patients with metastatic melanoma. *Journal of immunotherapy.* 2001;24(4):363-73.
2. Riddell SR, and Greenberg PD. The use of anti-CD3 and anti-CD28 monoclonal antibodies to clone and expand human antigen-specific T cells. *Journal of immunological methods.* 1990;128(2):189-201.
3. Tran E, Turcotte S, Gros A, Robbins PF, Lu Y-C, Dudley ME, Wunderlich JR, Somerville RP, Hogan K, and Hinrichs CS. Cancer immunotherapy based on mutation-specific CD4+ T cells in a patient with epithelial cancer. *Science.* 2014;344(6184):641-5.
4. Kreiter S, Selmi A, Diken M, Sebastian M, Osterloh P, Schild H, Huber C, Türeci Ö, and Sahin U. Increased antigen presentation efficiency by coupling antigens to MHC class I trafficking signals. *The Journal of Immunology.* 2008;180(1):309-18.
5. Engels B, Cam H, Schüler T, Indraccolo S, Gladow M, Baum C, Blankenstein T, and Uckert W. Retroviral vectors for high-level transgene expression in T lymphocytes. *Human gene therapy.* 2003;14(12):1155-68.
6. Sommermeyer D, Hudecek M, Kosasih PL, Gogishvili T, Maloney DG, Turtle CJ, and Riddell SR. Chimeric antigen receptor-modified T cells derived from defined CD8+ and CD4+ subsets confer superior antitumor reactivity in vivo. *Leukemia.* 2015.
7. Jones S, Peng PD, Yang S, Hsu C, Cohen CJ, Zhao Y, Abad J, Zheng Z, Rosenberg SA, and Morgan RA. Lentiviral vector design for optimal T cell receptor gene expression in the transduction of peripheral blood lymphocytes and tumor-infiltrating lymphocytes. *Human gene therapy.* 2009;20(6):630-40.
8. Lim CS, and Brown CM. Hepatitis B virus nuclear export elements: RNA stem-loop α and β, key parts of the HBV post-transcriptional regulatory element. *RNA biology.* 2016;13(9):743-7.
9. Kuball J, Dossett ML, Wolfl M, Ho WY, Voss R-H, Fowler C, and Greenberg PD. Facilitating matched pairing and expression of TCR chains introduced into human T cells. *Blood.* 2007;109(6):2331-8.
10. Li H. Aligning sequence reads, clone sequences and assembly contigs with BWA-MEM. *arXiv preprint arXiv:13033997.* 2013.
11. Li H, and Durbin R. Fast and accurate short read alignment with Burrows–Wheeler transform. *Bioinformatics.* 2009;25(14):1754-60.
12. McKenna A, Hanna M, Banks E, Sivachenko A, Cibulskis K, Kernytsky A, Garimella K, Altshuler D, Gabriel S, and Daly M. The Genome Analysis Toolkit: a MapReduce framework for analyzing next-generation DNA sequencing data. *Genome research.* 2010;20(9):1297-303.
13. Auwera GA, Carneiro MO, Hartl C, Poplin R, del Angel G, Levy-Moonshine A, Jordan T, Shakir K, Roazen D, and Thibault J. From FastQ data to high-confidence variant calls: the genome analysis toolkit best practices pipeline. *Current protocols in bioinformatics.* 2013:11.0. 1-.0. 33.

14. Bergmann EA, Chen B-J, Arora K, Vacic V, and Zody MC. Conpair: concordance and contamination estimator for matched tumor–normal pairs. *Bioinformatics.* 2016;32(20):3196-8.
15. Cibulskis K, Lawrence MS, Carter SL, Sivachenko A, Jaffe D, Sougnez C, Gabriel S, Meyerson M, Lander ES, and Getz G. Sensitive detection of somatic point mutations in impure and heterogeneous cancer samples. *Nature biotechnology.* 2013;31(3):213-9.
16. Saunders CT, Wong WS, Swamy S, Becq J, Murray LJ, and Cheetham RK. Strelka: accurate somatic small-variant calling from sequenced tumor–normal sample pairs. *Bioinformatics.* 2012;28(14):1811-7.
17. Koboldt DC, Zhang Q, Larson DE, Shen D, McLellan MD, Lin L, Miller CA, Mardis ER, Ding L, and Wilson RK. VarScan 2: somatic mutation and copy number alteration discovery in cancer by exome sequencing. *Genome research.* 2012;22(3):568-76.
18. Ramos AH, Lichtenstein L, Gupta M, Lawrence MS, Pugh TJ, Saksena G, Meyerson M, and Getz G. Oncotator: cancer variant annotation tool. *Human mutation.* 2015;36(4):E2423-E9.
19. Li B, and Dewey CN. RSEM: accurate transcript quantification from RNA-Seq data with or without a reference genome. *BMC bioinformatics.* 2011;12(1):323.
20. Chow I-T, Yang J, Gates TJ, James EA, Mai DT, Greenbaum C, and Kwok WW. Assessment of CD4+ T Cell Responses to Glutamic Acid Decarboxylase 65 Using DQ8 Tetramers Reveals a Pathogenic Role of GAD65 121–140 and GAD65 250–266 in T1D Development. *PloS one.* 2014;9(11):e112882.

Supplemental figures and tables:

Figure S1.

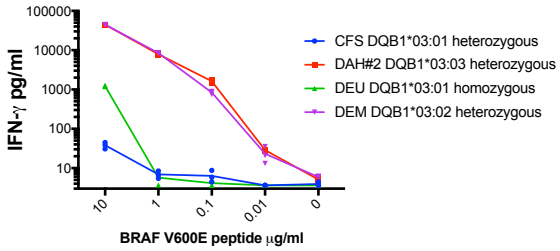

Figure S1

IFN-γ release by patient derived $BRAF^{V600E}$-specific T cells incubated with allogeneic B-LCL cell lines expressing HLA DQB1 03 alleles and pulsed with the indicated amount of 21-mer $BRAF^{V600E}$ peptide with 3 technical replicates.

Figure S2

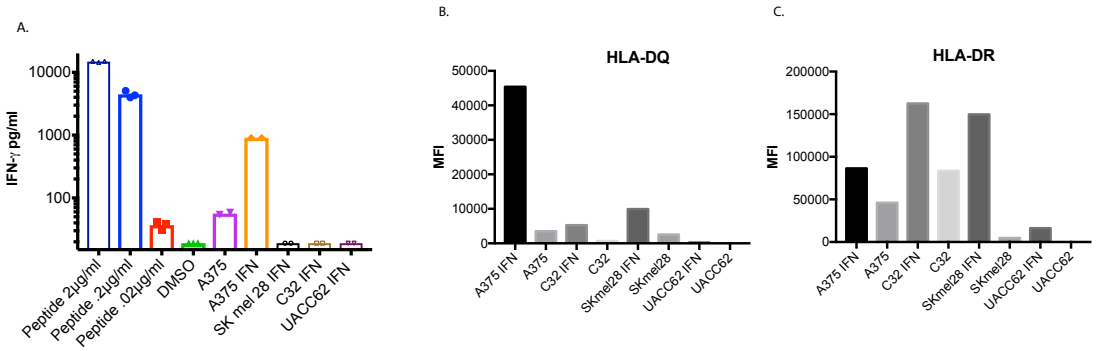

Figure S2.

A) IFN-γ release by patient derived $BRAF^{V600E}$-specific T cells incubated with autologous B cells pulsed with $BRAF^{V600E}$ peptide or the indicated tumor cell lines with and without pretreatment with human IFN-γ 500 U/ml for 3 days. 3 technical replicates were performed. B,C) Expression of HLA-DQ (B) and HLA-DR (C) on tumor cell lines with and without IFN-γ pre-treatment quantitated by flow cytometry relative to the isotype control.

Figure S3

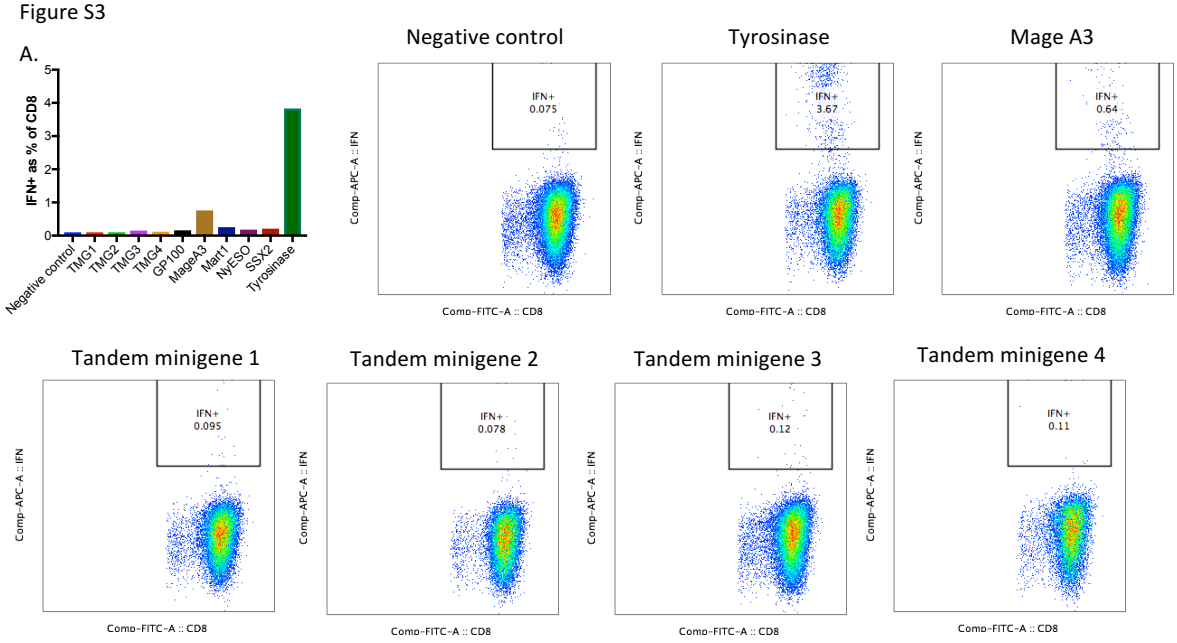

Figure S3.

Tumor infiltrating lymphocytes were incubated with autologous B cells transfected with tandem minigenes encompassing 29 non-synonymous mutations or the coding sequences from self antigens Tyrosinase, Mage A3, Mart1, SSX2, and GP100 in the presence of brefeldin A and IFN-γ production was measured in CD8+ T cells by intracellular cytokine staining.

Figure S4

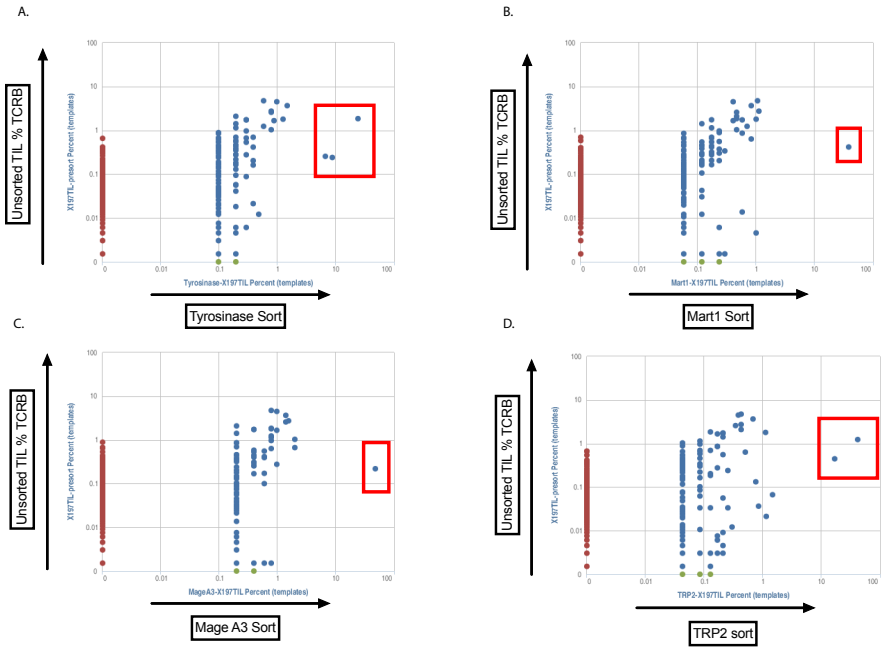

Figure S4.

TCRB sequencing on the TIL and T cells from TIL incubated with autologous B cells and tiled peptides spanning (A) Tyrosinase, (B) Mart1, (C) Mage A3, and (D) TRP2 and sorted by IFN-γ capture. Antigen specific TCRB sequences enriched in the sorted cells are marked with a red box.

Symbol	Chrm	Pos	Nucleotide	Amino Acid			Ref #	Alt #	VAF	27-mer amino acid sequence	Mutation in DNA	Mutation in RNA	20-mer peptide 1	20-mer peptide 2	TPM in RNA
AP1M1	chr19	16339014	AP1M1.A>C	p.I295L	A	C	240	67	21.8%	VIEKHSHSRIEYMLKAKSQFKRRSTAN	yes	yes	VIEKHSHSRIEYMLKAKSQF	SRIEYMLKAKSQFKRRSTAN	61.33
BRAF	chr7	140453136	BRAF.A>T	p.V600E	A	T	31	17	35.4%	DLTVKIGDFGLATEKSRWSGSHQFEQL	yes	yes	DLTVKIGDFGLATEKSRWSG	DFGLATEKSRWSGSHQFEQL	10.83
DCAF6	chr1	167973908	DCAF6.G>A	p.A419T	G	A	52	74	58.7%	EQFLQPSTSSTMSTQAHSTSSPTESPH	yes	yes	EQFLQPSTSSTMSTQAHSTS	TSSTMSTQAHSTSSPTESPH	41.11
GTF2H4	chr6	30879921	GTF2H4.C>T	p.T319M	C	T	108	16	12.9%	FIVVETNYRLYAYMESELQIALIALFS	yes	yes	FIVVETNYRLYAYMESELQI	YRLYAYMESELQIALIALFS	49.95
NBPF12	chr1	146450115	NBPF12.A>G	p.E2471G	A	G	35	25	41.7%	DSCQPYRSSFYALGEKHVGFSLDVGEI	yes	yes	DSCQPYRSSFYALGEKHVGF	SSFYALGEKHVGFSLDVGEI	12.5
ORC3	chr6	88318940	ORC3.A>C	p.I236L	A	C	27	5	15.6%	ESFATKVLQDFIILSSQHLHEFPLILI	yes	yes	ESFATKVLQDFIILSSQHLH	LQDFIILSSQHLHEFPLILI	19.92
ROR1	chr1	64475043	ROR1.A>G	p.N53S	A	G	33	25	43.1%	LVPTSSWNISSELSKDSYLTLDEPMNN	yes	yes	LVPTSSWNISSELSKDSYLT	NISSELSKDSYLTLDEPMNN	4.69
SF3B1	chr2	198273138	SF3B1.T>C	p.T358A	T	C	29	7	19.4%	QMGGSTPVLTPGKAPIGTPAMNMATPT	yes	yes	QMGGSTPVLTPGKAPIGTPA	VLTPGKAPIGTPAMNMATPT	105.2
UNKL	chr16	1453173	UNKL.C>T	p.V154I	C	T	50	32	39.0%	AHGPLDLRPPVCDIRELQAQEALQNGQ	yes	yes	AHGPLDLRPPVCDIRELQAQ	RPPVCDIRELQAQEALQNGQ	6.72
ZNF700	chr19	12059700	ZNF700.T>G	p.F287L	T	G	68	20	22.7%	GEKPYECSKCDKALHSSSSYHRHERSH	yes	yes	GEKPYECSKCDKALHSSSSY	SKCDKALHSSSSYHRHERSH	8.69
NVL	chr1	224484275	NVL.T>G	p.T370P	T	G	37	13	26.0%	APCIIFIDEIDAIPPKREVASKDMERR	yes	yes	APCIIFIDEIDAIPPKREVA	DEIDAIPPKREVASKDMERR	18.42
MATN1	chr1	31191789	MATN1.T>G	p.T153P	T	G	47	62	56.9%	SRSPDISKVVIVVPDGRPQDSVQDVSA	yes	yes	SRSPDISKVVIVVPDGRPQD	KVVIVVPDGRPQDSVQDVSA	0.14
CTNNA2	chr2	80136918	CTNNA2.A>C	p.N351H	A	C	139	32	18.7%	VRQALQDLLSEYMHNTGRKEKGDPLNI	yes	no	VRQALQDLLSEYMHNTGRKE	LLSEYMHNTGRKEKGDPLNI	2.36
GET4	chr7	925731	GET4.T>G	p.L65R	T	G	148	47	24.1%	RYMSQSKHTEARERMYSGALLFFSHGQ	yes	no	RYMSQSKHTEARERMYSGAL	HTEARERMYSGALLFFSHGQ	26.97
NTNG1	chr1	107867468	NTNG1.G>A	p.V271I	G	A	26	26	50.0%	TVTDLRIRLLRPAIGEIFVDELHLARY	yes	yes	TVTDLRIRLLRPAIGEIFVD	RLLRPAIGEIFVDELHLARY	0.73
SPTBN5	chr15	42147465	SPTBN5.G>A	p.T3127I	G	A	113	52	31.5%	TLLLDAWLTTKAAIAESQDYGQDLEGV	yes	yes	TLLLDAWLTTKAAIAESQDY	LTTKAAIAESQDYGQDLEGV	1.11
DPP6	chr7	154143393	DPP6.C>T	p.S113L	C	T	33	24	42.1%	LLVILVICSLIVTLVILLTPAEDNSLS	yes	no	LLVILVICSLIVTLVILLTP	CSLIVTLVILLTPAEDNSLS	0.03
HIAT1	chr1	100525467	HIAT1.G>T	p.G93C	G	T	19	7	26.9%	VKGLLSFLSAPLICALSDVWGRKSFLL	yes	no	VKGLLSFLSAPLICALSDVW	LSAPLICALSDVWGRKSFLL	46.71
ITGA4	chr2	182350641	ITGA4.G>T	p.V359F	G	T	55	16	22.5%	GSGAVMNAMETNLFGSDKYAARFGESI	yes	no	GSGAVMNAMETNLFGSDKYA	AMETNLFGSDKYAARFGESI	4.59
MYO1A	chr12	57422622	MYO1A.C>T	p.V1017I	C	T	95	31	24.6%	SVRFKENSVAVKVIQGPAGGDNSKLRY	yes	no	SVRFKENSVAVKVIQGPAGG	SVAVKVIQGPAGGDNSKLRY	0.05
B4GALT5	chr20	48257072	B4GALT5.T>G	p.Y246S	T	G	81	7	8.0%	HDVDHIPESDRNYSGCGQMPRHFATKL	yes	yes			45.21
ITCH	chr20	33045210	ITCH.G>A	p.S450N	G	A	41	4	8.9%	LGPLPPGWEKRTDNNGRVYFVNHNTRI	yes	no			23.48
KMT2B	chr19	36220941	KMT2B.T>G	p.F1664C	T	G	144	9	5.9%	VGCCLSSCLSNFHCMCARASYCIFQDD	yes	no			12.6
SMC1B	chr22	45749929	SMC1B.G>T	p.Q1068K	G	T	40	4	9.1%	FEQVKKRRYDLFTKCFEHVSISIDQIY	yes	no			0.57
SPG11	chr15	44877944	SPG11.G>T	p.H1671N	G	T	46	3	6.1%	HTIITSYSIENLQNECRSILERLQTDG	yes	no			19.43
ZNF148	chr3	124953119	ZNF148.T>C	p.H241R	T	C	13	3	18.8 %	RCDECGMRFIQKYRMERHKRTHSGEKP	yes	no			7.62
ZNF658	chr9	40774255	ZNF658.A>C	p.H340Q	A	C	103	7	6.4%	SNKCEENFSQSSAQIVHQKTQAGDKFG	yes	yes			2.76
USP2	chr11	119230366	USP2.A>C	p.F277C	A	C	153	9	5.6%	QGLAGLRNLGNTCCMNSILQCLSNTRE	yes	yes			7.03
SLC19A3	chr2	228560627	SLC19A3.T>G	p.M384L	T	G	46	5	9.8%	ACYAGYLIFKSSYLLLITIAVFQIAVN	yes	no			2.34

Table S1

Nonsynonymous mutations in patient melanoma identified by whole exome sequencing and peptides used in subsequent experiments. Annotations include chromosomal position using GRCh37/hg19 reference assembly, nucleotide and amino acid substitutions, whether the mutation was observed in DNA or RNA-seq, the variant allele frequency (VAF), and RNA-seq expression in units of transcripts per million (TPM).

Cell line name	BRAF V600E Peptide	Mean IFN-G pg/ml		HLA DRB1	HLA DQB1
1331	-	10		404	302
	+	41791			
CFS	-	10		0401, 0101	0301, 0501
	+	1547			
DEM	-	23		0401, 1602	0302, 0502
	+	29873			
DEU	-	6		401	301
	+	10359			
FAL	-	9		0403, 0801	03BG, 0402
	+	31620			
BM14	-	536		401	302
	+	42832			
DMB	-	38		0101, 1501	0501, 0602
	+	7			
DLM	-	26		0403, 0801	03BG, 0402
	+	39388			
AMM	-	6		0802, 1501	0402, 06WG
	+	9			
CLC	-	9		0301, 1104	02AB, 0301
	+	6			
BP	-	35		1601, 1101	0502, 0301
	+	36			
JWP	-	12		0701, 0701	02AB, 0303
	+	359			
DAH2	-	17		09, 1501	0303, 06W6
	+	49784			
VRM	-	6		0701, 10	0303, 0501
	+	188			

Table S2

IFN-γ production by patient $BRAF^{V600E}$-specific $CD4^+$ T cells after incubation with allogeneic B-LCL cell lines expressing different HLA class II alleles, alone or pulsed with 10 μg/ml of $BRAF^{V600E}$ peptide. The complete patient HLA typing was as follows:

A*11:01:01/A*24:02:01

B*15:01:01/B*40:01:02

C*03:03:01/C*03:04:01

DPA1*01:03:01/DPA1*01:03:01

DPB1*04:01:01/DPB1*04:01:01

DQA1*03:01:01/DQA1*03:02

DQB1*03:02:01/DQB1*03:03:02

DRB1*04:03:01/DRB1*09:01:02

DRB4*01:03:01/DRB4*01:03:02

Table S3 Phenotype of final TIL product

% of live	% of CD45					
CD45	CD3 T	γδ T	NKT	CD8 T	CD4 T	Treg
99.9	99.7	0.04	0.014	93.9	3.4	0.52
% of CD45						
CD8 PD1	CD8 TIM3	CD8 CM	CD8 naïve	CD8EMRA	CD8EM	
51.6	93.4	0.002	0.003	36.5	58.6	
% of CD8 or CD4						
CD8 INFg	CD4 IL17+	CD4 IL22	CD4 IFNg+			
99.3	3.6	0.42	98.8			

Table S3.

The final TIL product infused into the patient was analyzed by flow cytometry for phenotype and following stimulation with PMA/Ionomycin was stained intracellularly for cytokines. Percentages are percentages of CD45+ cells (top) or CD4 or CD8 Cells (bottom).

Table S4 Tumor specificity and class I blocking of initial TIL cultures

	Pool T	Pool R	Pool B	Pool A	Pool S	Pool 1	Pool 2	Pool 3	Pool 4	Pool 5	Pool 6	Fragment 12
Tumor	2179.50	752.12	2993.64	4427.63	2313.73	3409.99	7213.00	3722.50	3866.23	2914.58	3916.23	2.44
Tumor + Class I Block	94.32	11.95	67.49	38.78	67.88	75.74	394.68	258.88	86.28	369.32	513.78	2.44
Media only	2.44	52.71	67.56	2.44	2.44	40.87	16.52	131.40	2.44	2.44	21.22	2.44
PMA/Iono	2010.14	360.33	2563.22	2929.14	1203.62	2038.37	1565.83	1454.78	2757.56	2012.09	2155.09	2.44
Percent Blocking	96%	98%	98%	99%	97%	98%	95%	93%	98%	87%	87%	0%

Table S4

TIL cultures derived from independent tumor fragments were incubated with a single cell suspension of autologous tumor in the presence or absence of class I HLA blocking antibody, and IFN-γ release was measured by ELISA.

Table S5

Individual TCRB clones with indicated CDR3 nucleotide sequences and their template frequency given as a percentage of total TCRB templates within the indicated samples. Self-antigen reactive CD8 clones are indicated in yellow, BRAF V600E reactive CD4 clones are indicated in blue, and the remainder of the top 34 TCRB clones in the TIL product are shown in green.